AN INNOVATIVE INDUCTIVE AIR-GAP MONITORING SYSTEM FOR LARGE LOW SPEED HYDRO-GENERATORS, TESTS IN OPERATION

Jean-Jacques Simond, Mai Tu Xuan, Roland Wetter
Swiss Federal Institute of Technology, EPFL-STI-IEL-LME
Station 11, CH-1015 Lausanne, Switzerland
Tel.: (+41) 21 693 4804 - Fax: (+41) 21 693 2687
e-mail: jean-jacques.simond@epfl.ch

ABSTRACT

Large low speed hydro-generators (fig. 1) have a very small specific air-gap to stator bore diameter ratio making it virtually impossible to have a perfect centering of the rotor within the stator during the assembly process. Therefore the machines are operated with an eccentricity that, though small, is not negligible, and is the cause of undesirable effects: considerable unbalanced magnetic pulls, vibrations, additional losses. It is therefore important to assess the eccentricity and even more to check its trend in case of any stator or rotor deformations in order to guarantee a safe operation and to prevent any serious damage at an early stage.

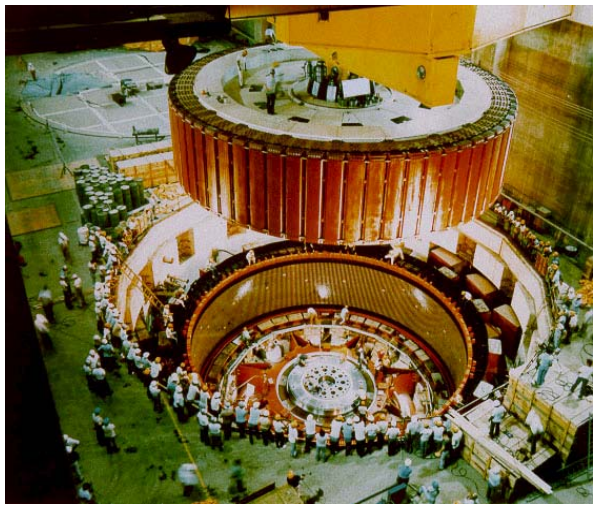

Fig. 1: Large low speed hydro-generator.

This paper describes a novel and patented [1] air-gap monitoring system for large low speed synchronous hydro-generators. This new system is based on inductive sensors made of simple coils distributed on the periphery of the stator, each one between two ventilation ducts. These coils may be put in place by the manufacturer; for generators already in operation, the coils are put in place from the back of the stator yoke using a simple method. It does not require an access to the rotor; of course the coils are easy to remove.

KEYWORDS: air-gap monitoring, bearing clearance, eccentricity, magnetic pull, preventive maintenance.

I INTRODUCTION

The purpose of the EDP Monitoring device (Eccentricities, Deformation and Unbalanced magnetic pull Monitoring) is to detect synchronous machine stator and rotor circuit defects. These defects, of mechanical origin (wrong positioning of the rotor, mechanical unbalance, mechanical deformation…) or electromagnetic origin (partial short circuit in field coils, magnetic circuit defect…), may engender important magnetic strains between the stator and the rotor giving rise to vibrations and in the worst case a rubbing of the rotor and the stator. Early detection of air-gap anomalies eases the maintenance task by giving the user time to plan for repairs before scheduled outages. Prediction of long term evolution of air-gap, stator and rotor shape can be used in operational and rehabilitation planning. Knowing the magnitude of the magnetic pull between rotor and stator can inform the operator of the need to remove a machine from service before serious damage such as a rotor stator rub occurs.

Recent and unpublished results obtained on large machines as well as on a laboratory prototype machine are presented, they confirm the advantages of this new monitoring system in terms of performances and costs compared to the capacitive air-gap monitoring solutions available these days on the market [3,4].

II. MEASUREMENT EQUIPMENT

The EDP device is based on the measurements of the induced voltages in air-gap sensors. This system is able to calculate in real time a static or a dynamic rotor eccentricity, a stator or a rotor deformation, a partial short-circuit in the field winding. It determines also the unbalanced magnetic pulls in magnitude and direction by taking into account not only the saturation level in the magnetic main circuit but also the different damping effects due to the currents in parallel paths and equipotential connections of the stator winding and, in the case of a static eccentricity, due to the damper winding. This paper focuses on a description of this new air-gap monitoring system and shows practical measurement results, the physical theoretic basis is explained in [2] and summarized in appendix.

The measurement equipment is shown in fig. 2.

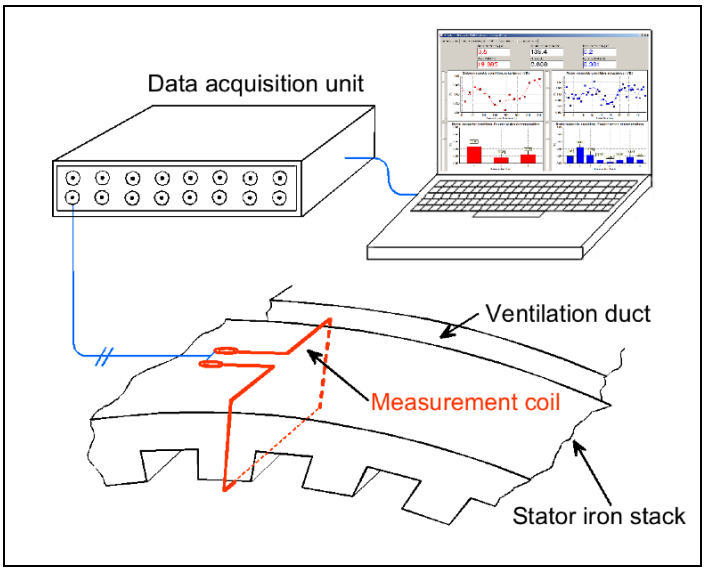

Fig. 2. UMP Monitoring equipment.

It consists of:

- Measurement coils put in place on the periphery of the stator stack, each coil between two ventilation ducts (fig. 3).
- A data acquisition unit.
- A PC for the processing, leading from the sensor induced voltages to the static and dynamic eccentricities, to the rotor and stator mechanical deformations and to the unbalanced magnetic pulls.

Fig. 3.: Sensor in a 128 MVA generator.

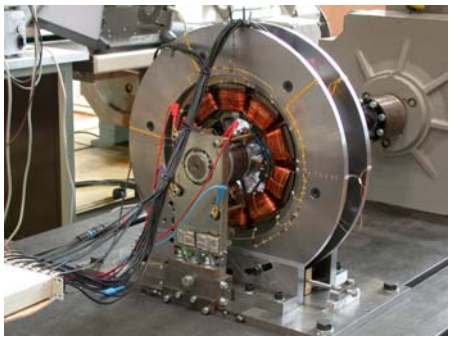

Fig. 4.: Laboratory prototype machine.

III. EXAMPLES OF APPLICATION

The applications presented in this section concern two machines, whose rated values are given in table 1. The first one is a unit of the Verbois hydropower plant in Geneva.

	Lab prototype	Verbois Unit 2
Rated power [MVA]	0.020	33
Rated voltage [kV]	0.380	9
Frequency [Hz]	50	50
Number of poles	10	44

Table 1: Rated values of the two machines

The second one is a laboratory prototype machine with the following special features (fig. 4). A mechanical bearing positioning system allows any 1st order static eccentricity of the rotor; the higher orders of a static eccentricity correspond to a stator bore deformation (see appendix). The insertion of iron sheets under the pole shoes leads to any dynamic eccentricity of the rotor. A 1st order dynamic eccentricity appears in a machine with circular stator bore and rotor when the rotor centre O' is different as the stator centre O and rotates with respect to O at the machine rotating speed. The higher orders of a dynamic eccentricity correspond to a rotor deformation. Three stators are available. The original one with a three phase winding comprising parallel current paths and equipotential connections. The two others with an elliptical (2nd order static eccentricity), respectively with a triangular (3rd order static eccentricity) slot less shape (fig. 4). All stators are equipped with 15 sensors.

A. Applications to the laboratory test machine

Fig. 5 shows a test result on the prototype machine at rated flux and synchronous speed. The stator bore is triangular; the rotor has a static eccentricity and the pole no 8 is adjusted off centre. 15 sensors are used on the periphery of the stator. The three defaults mentioned are perfectly visible on fig. 5. In this test the static rotor eccentricity and the triangular stator bore correspond to the stator 1st and 3rd deformation orders.

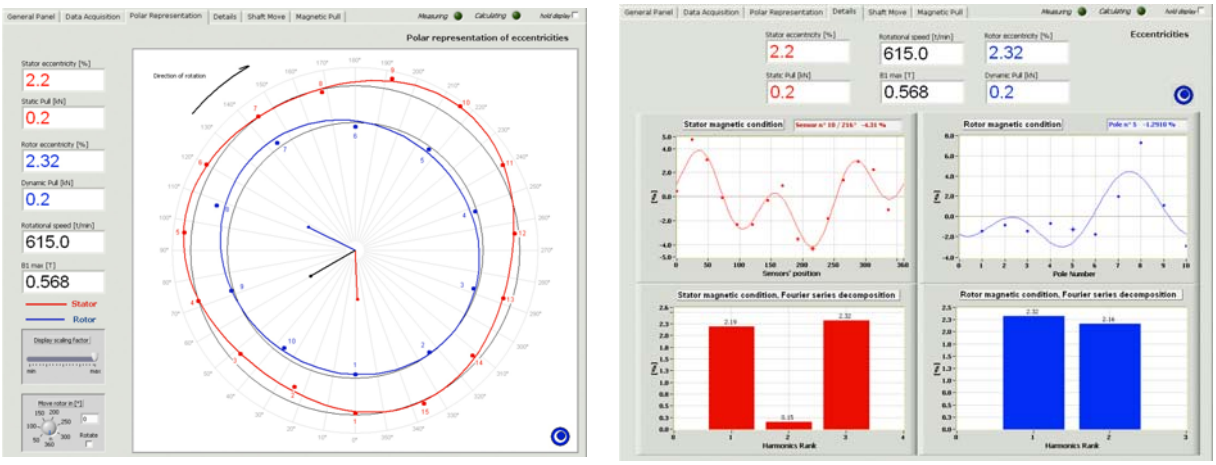

Fig. 5: Laboratory prototype, triangular stator, static eccentricity, pole 8 adjusted off centre.
Polar representation and Fourier analysis.

Table 2 compares results obtained with the original stator winding. The rotor has a 1st order static eccentricity of about 8% and a 1st order dynamic eccentricity of about 13%. Three cases are analysed: without parallel current paths in the stator winding (detailed results in fig. 6), with parallel current paths, with parallel current paths and equipotential connexions.

The results in table 2 clearly confirm the strong damping effect of a stator winding with parallel current paths and equipotential connections on the relative static and dynamic eccentricities and consequently on the unbalanced magnetic pulls. This damping effect is due to the fact that a stator or a rotor deformation of order N produces parasitic rotating induction waves with p±N pole pairs inducing the stator parallel current paths, these latter play the role of a stator damper winding. A damping effect is produced by the damper winding but only on parasitic induction waves produced by the static eccentricity.

Case	Static eccentricity	Dynamic eccentricity.	Static pull [kN]	Dynamic pull [kN]
Test 1: no stator damping	7.7 %	12.3 %	0.6	0.9
Test 2: parallel circuits	1.9 %	4.5 %	0.14	0.33
Test 3:parallel circuit + equipot.	0.6 %	1.5 %	0.04	0.11

Table 2: Eccentricity measurements with and without stator damping.

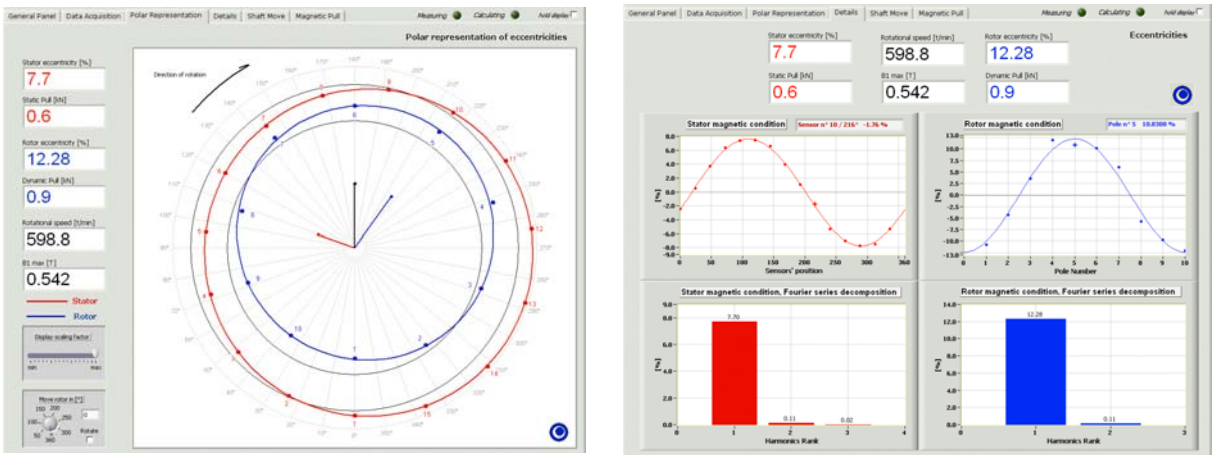

Fig. 6: Laboratory prototype, original stator, mixed eccentricity, no stator damping.

B. Applications to the unit 2 of Verbois

In the real case of an existing unit, the possible stator and rotor deformations do not correspond to the simple definitions given before for the static and dynamic eccentricities. These deformations contain harmonics orders bigger than 1 or 2. Knowing that the measurement of a deformation harmonic order N requires at least 5·N sensors, it is economically primordial to use low cost sensors like those described in this paper. *Fig. 7 illustrates the risk of errors using a too low number of inductive or capacitive sensors: the case of fig. 7a) leads to different results for the same deformation, the case of fig. 7b) leads to non existing eccentricity and unbalanced magnetic pull. The minimal number of sensors required for the two examples in fig. 7 is 20, respectively 15.*

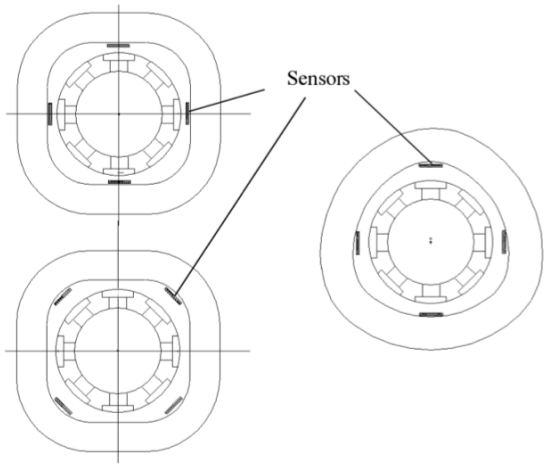

Fig. 7: Configurations with only 4 sensors.

Unit 2 has been measured under rated load conditions using 16 sensors. Fig. 8 illustrates the results obtained. The static (0.9%) and the dynamic (0,76%) eccentricities obtained indicate that this unit has almost perfect stator bore, rotor and air-gap geometries.

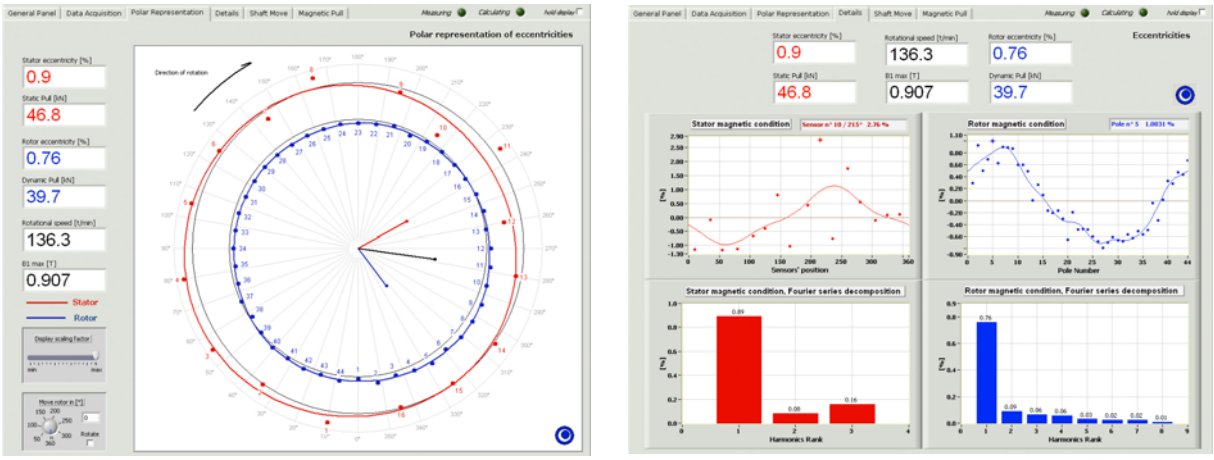

Fig. 8: Verbois, unit 2, measurement under rated load with 16 sensors.

IV. DETECTION OF BEARING CLEARANCES

In the previous paragraphs the stator bore and rotor deformations considered had already been defined on a very general way; nevertheless these deformations were not time dependent, in others words the fundamental period was equal to one machine revolution. The next step is now to take into account a possible clearance in the bearings leading to a possible shaft movement. The period of such a shaft movement is hazardous and surely higher than one machine revolution. ***The idea is to try to use the algorithms developed before in order to recognize in a given case if a shaft movement and consequently a bearing clearance exits or not. In case a shaft movement exists, its amplitude should be estimated.*** This control is of course extremely important for the machine's user and should be detected as soon as possible in order to guarantee a reliable machine operation.

The first harmonic of the static eccentricity represents the permanent displacement between the centre points of the stator and of the rotor; it corresponds to the first order of the spatial Fourier analysis in fig. 5 “stator magnetic condition”. In case of a shaft movement, this first harmonic is different for two successive machine revolutions. If the Fourier analysis is performed over a high number of machine revolutions corresponding to the fundamental period of the shaft movement, the shaft movement is filtered out of the result obtained. Due to the fact that the fundamental period of the shaft movement is unknown in practice, the Fourier analysis has to be performed over a high number of machine revolution (about 50), the first harmonic obtained over this high number of revolutions is then very far to the first harmonic obtained in case of the fundamental period of the shaft movement were known.

A shaft movement can be identified through the first harmonic of the dynamic eccentricity according to the time Fourier analysis in fig. 5 “rotor magnetic condition” on the following manner. Over a high number N of machine revolutions a determination of the dynamic eccentricity is started systematically after a rotation of one pole over one machine revolution.

Each successive determination n° i of the dynamic eccentricity leads to a first harmonic $\underline{^1\varepsilon_{dyn,i}}$. This first harmonic contains the first harmonic we had without a shaft movement and the shaft movement. The first harmonic $\underline{\delta_d}$ calculated on the N machine revolutions doesn’t contain the shaft movement anymore. Therefore the shaft movement can be estimated versus time by:

$$\underline{\delta} = \underline{^1\varepsilon_{dyn,\,i}} - \underline{\delta_d}$$

$\underline{\delta}$ is illustrated in polar representation in fig. 9 in case of a large vertical hydro-generator affected by a noticeable guide bearing clearance. This representation is given in two measurements planes (top and bottom planes of this vertical unit). It is therefore possible to get a precise idea of the time dependent machine axis obliquity appearing consequently to the clearances of the bearings.

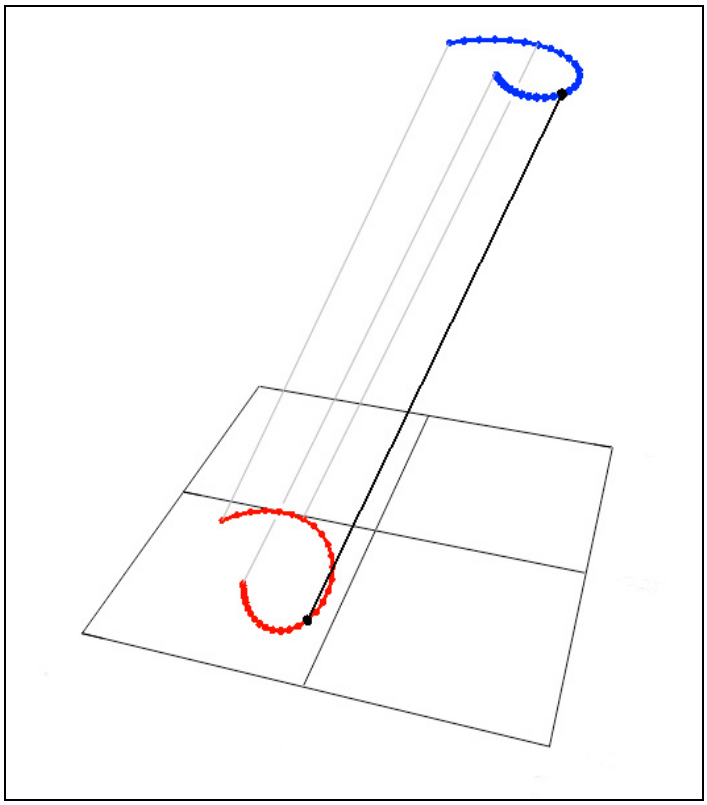

Fig. 9: δ measurement in case of bearing clearances.

V. CONCLUSIONS

A new air-gap monitoring system based on low cost inductive sensors has been presented; its major benefits versus a capacitive air-gap monitoring system are the following**:**

Performances: Possibility to measure separately stator and rotor magnetic circuits’ deformation shapes till order N when using 5·N low cost inductive sensors. Measurement of magnitude and phase of the static and dynamic unbalanced magnetic pulls. Possible detection of a partial short-circuit inside the excitation winding.

Measuring equipment: The low cost inductive sensors used are extremely simple and easy to install and to remove; they are also completely insensitive to humidity and

temperature conditions. Neither a direct access to the air gap, nor gluing are required. The necessary data acquisition unit and the PC are available on the market. Induced voltages are measured in an unproblematic range between 1 and 5 V.

The performances of this new air-gap monitoring system have been successfully checked on a laboratory prototype machine and on several large units.

BIBLIOGRAPHICAL REFERENCES

[1] M. TU XUAN, J.-J. SIMOND, *Procédé et dispositif de traitement de signaux pour la détection des défauts des circuits magnétiques statorique et rotorique d'une machine synchrone*. European Patent PCT/CH2004/00101 (Feb. 2004), EP 03004796.3 (2003).

[2] M. TU XUAN, J.-J. SIMOND, R. WETTER, S. KELLER, June 2006. *A Novel Air-Gap Monitoring System For Large Low Speed Hydro-Generators*. IEEE, PES annual meeting, Canada, Montreal.

[3] M. BISSONNETTE. M. CLOUTIER, 1989. *Air gap measuring syste*m. Proceedings of the 1st International Machinery Monitoring and Diagnostic Conference, USA, Las Vegas, Nevada, pp. 261-267.

[4] G.B. POLLOCK, J.F. LYLES, Dec. 1992. *Vertical hydraulic generators experience with dynamic air gap monitoring*. IEEE Transactions on Energy Conversion, vol. 7, no. 4, pp. 660-668, USA.

APPENDIX

The harmonic components of the air-gap flux density for a machine without eccentricity, at synchronous speed Ω and in a stator reference frame is given by equation (1):

$$B_i(\alpha_r) = \sum_{\upsilon} {}^{\upsilon}B_{\max} \cdot \sin(\upsilon \cdot \alpha_r + {}^{\upsilon}\varphi_B) \quad (1)$$

where ${}^{\upsilon}B_{\max}$ and ${}^{\upsilon}\varphi_B$ are amplitude and phase angle of the harmonic component with order υ, α_r is the angle in a rotor reference frame.

The stator bore deformations and a static eccentricity can be written by means of a modulation function $\Lambda_a(\alpha_s)$:

$$\Lambda_a(\alpha_s) = 1 + \sum_{\eta} {}^{\eta}\Lambda_{a\max} \cdot \sin(\eta \cdot \alpha_s + {}^{\eta}\varphi_{\Lambda a}) \quad (2)$$

and the rotor deformations, a dynamic eccentricity or a partial short-circuit in the field winding by means of a modulation function $\Lambda_r(\alpha_s)$:

$$\Lambda_r(\alpha_s) = 1 + \sum_{\kappa} {}^{\kappa}\Lambda_{r\max} \cdot \sin\left[\kappa \cdot (\alpha_s - \Omega \cdot t) + {}^{\kappa}\varphi_{\Lambda r}\right] \quad (3)$$

where ${}^{\eta}\Lambda_{a\max}$ and ${}^{\kappa}\Lambda_{r\max}$ are the amplitudes of the stator and rotor deformation harmonics with orders η and κ, ${}^{\eta}\varphi_{\Lambda a}$ and ${}^{\kappa}\varphi_{\Lambda r}$ are the phase angles of the stator and rotor deformation harmonics with orders η and κ.

The goal of the proposed UMP monitoring strategy is to measure these two modulation functions. The combination of equations (1), (2) and (3) leads to the air-gap flux density distribution $B(\alpha_s,t)$ for a machine with an eccentricity and any kind of stator or rotor deformations:

$$B(\alpha_s,t) = B_i(\alpha_s,t) \cdot \Lambda_a(\alpha_s) \cdot \Lambda_r(\alpha_s) \quad (4)$$

The air-gap flux density $B(\alpha_s,t)$ is seen by the sensor put in place on the stator at the position

α_s. The induced voltage in this coil is given by:

$$u_i = B(\alpha_{si}) \cdot v \cdot L \tag{5}$$

where v is the tangential rotor speed and L the axial length of the coil.

Fig. 10a illustrates an example of three induced voltages u_i in three sensors placed on the stator at the positions α_{si}.

A low pass filter, eliminating the harmonic orders with a frequency higher than the rated frequency, leads to the filtered induced voltage u_{fi} in the coil number i (fig. 10b). The envelopes e_i of the u_{fi} voltages and their time mean values e_{im} are represented in fig. 11 for one machine rotation. Fig. 11 also shows the spatial mean value e_{ms} of the time mean values e_{im} of all measurement coils put in place on the stator.

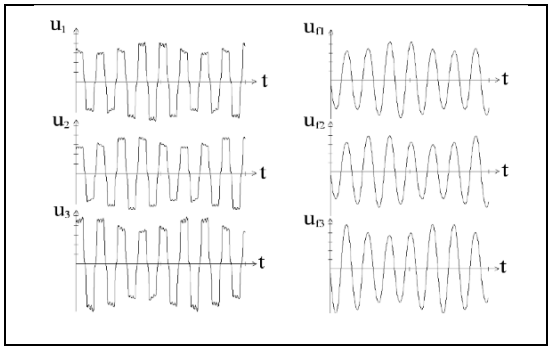

a)

Fig. 10: Induced voltages u_i before and u_{fi} after filtering in three measurement coils

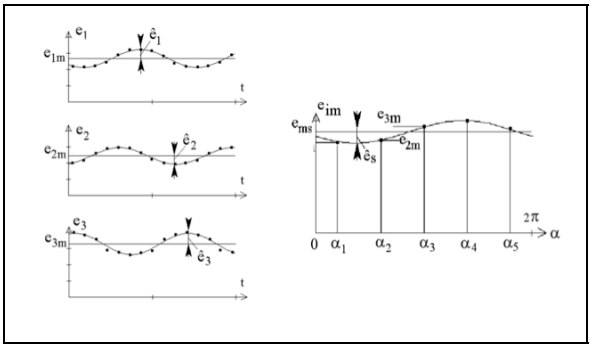

b)

Fig. 11: Envelopes of the u_{fi} voltages, spatial mean value e_{ms} of the time mean value e_{im}.

The functions e_i, e_{im} and the mean value e_{ms} can be obtained with the described monitoring system; using them, it is possible to get the two modulation functions according to the equations (2) and (3) and therefore all information concerning the eccentricities as well as any stator and rotor deformations [2]:

$$\Lambda_a(\alpha_s) = 1 + \sum_{\eta} {}^{\eta}\Lambda_{a\max} \cdot \sin(\eta \cdot \alpha_s + {}^{\eta}\varphi_{\Lambda a}) = \frac{e_{im}}{e_{ms}} \tag{6}$$

$$\Lambda_r(\alpha_s) = 1 + \sum_{\kappa} {}^{\kappa}\Lambda_{r\max} \cdot \sin\left[\kappa \cdot (\alpha_s - \Omega \cdot t) + {}^{\kappa}\varphi_{\Lambda r}\right] = \frac{e_i}{e_{im}} \tag{7}$$

One observes that the $\Lambda_r(\alpha_s)$ function is the same for all measurement coils. That means that $\Lambda_r(\alpha_s)$ can be obtained using only one measurement coil.

Finally, knowing the air-gap flux density distribution, it is easy to calculate the magnetic pressure σ between stator and rotor:

$$\sigma(\alpha_s) = \frac{B^2(\alpha_s)}{2 \cdot \mu_0} \tag{8}$$

and the resulting magnetic force F on a portion or on the totality of the bore:

$$F = L \cdot R \cdot \int_{\alpha_1}^{\alpha_2} \sigma \cdot d\alpha \tag{9}$$

where L is the active length of the machine and R the bore radius.